

Passive Treatment of Acid Mine Drainage Integrated with Carbon Dioxide Removal by Enhanced Rock Weathering in Acid Mine Drainage

Fugo Nakamura¹, Hkaung Htut San¹, Hajime Iwaki¹, Monthicha Rawangphai¹, Naomi Kitagawa², Shinichiro Morimoto², Takao Nakagaki³, Tsutomu Sato¹

¹Laboratory of Eco-Materials and Resources, Course of Sustainable Resources Engineering, School of Engineering, Hokkaido University

²Environmental and Social Impact Assessment Team, Global Zero Emission Research Center, The National Institute of Advanced Industrial Science and Technology, Department of Energy and Environment

³Nakagaki Laboratory, Department of Mechanical Engineering, School of Creative Science and Engineering, Waseda University

Abstract

Interest is growing in Enhanced Rock Weathering (ERW) as a Carbon Dioxide Removal (CDR) strategy already applied to terrestrial and marine environments. Research shows that most silicate minerals dissolve several orders of magnitude faster under strongly acidic conditions like those found in acid mine drainage (AMD). An advantage of this approach is that silicate mineral dissolution from basalt increases AMD pH, potentially enabling passive treatment systems. To investigate both CDR potential and passive treatment possibilities of basalt-based ERW in AMD, we conducted one-dimensional reactive-transport modeling (1D-RTM) as a case study using the Amemasu River downstream from the abandoned Shojin mine. Using 1D-RTM, we estimated annual basalt weathering rates, CDR potential, and secondary schwertmannite formation. Life cycle assessment (LCA) and techno-economic evaluation (TEA) were then performed to determine net CDR and economic feasibility. We applied a surface complexation model (SCM) to evaluate contaminant adsorption by schwertmannite precipitates. Results show that ERW in AMD provides sufficient net CDR to be economically viable. Moreover, schwertmannite formation efficiently removes arsenic through adsorption while simultaneously releasing protons that maintain the acidic conditions necessary for enhanced mineral weathering. These dual benefits—carbon sequestration and contaminant removal—offer substantial economic incentives for treating AMD sites, particularly those contaminated with arsenic, iron, and sulfate. AMD treatment with limestone can be a major challenge to carbon neutrality in terms of economic burden and emissions. Our findings suggest the possibility of replacement of some active AMD treatment with limestone.

Keywords: ERW, CDR, 1D-RTM, SCM, LCA/TEA, schwertmannite

Introduction

The urgent need for cost-effective AMD treatment has driven interest in passive remediation approaches that utilize natural attenuation processes. In AMD treatment using limestone, the reaction of limestone with acid emits CO₂ gas. As limestone is

the most common neutralizing agent, if carbon pricing is imposed on limestone-derived CO₂ emissions, its cost may rise, further increasing the economic burden of AMD treatment. Meanwhile, Enhanced Rock Weathering (ERW) is emerging as a promising Carbon Dioxide Removal (CDR) technology for carbon neutrality. Current



ERW applications focus on agricultural and marine sites with moderately acidic to alkaline environments.

Studies show that most silicate minerals dissolve much faster in strongly acidic environments such as AMD. Fig. 1 illustrates the relationship between the dissolution rate of major minerals in basalt and pH. For example, labradorite, an abundant mineral in basalt, dissolves approximately 1000 times faster at pH 2 compared to pH 7. This pH-dependent dissolution behavior suggests that applying ERW to strongly AMD could dramatically enhance mineral weathering rates. Moreover, adding basalt could enable passive treatment, continuously removing harmful elements while meeting wastewater standards. In our case study, we conducted geochemical modeling, life cycle assessment (LCA), and techno-economic assessment (TEA) of ERW in the Amemasu River, an AMD-affected river in Hokkaido where our research group is conducting field experiments, and our study clarified the effectiveness of ERW regarding both CDR and passive AMD treatment.

Methods

Modeling concept

This study evaluates CDR through the following steps. Basalt powder added to AMD releases cations (Ca, Mg, Na, K) while simultaneously removing sulfate

ions through schwertmannite formation. Following the reaction, the treated river water enters the ocean, enhancing alkalinity without further basalt dissolution or schwertmannite formation. Total alkalinity is directly proportional to the concentration of dissolved inorganic carbon (DIC) because increased ocean alkalinity enhances CO_2 dissolution, raising dissolved inorganic carbon (DIC) concentrations. This relationship, defined by the proportionality constant η , is represented in Equation 1. Here ΔA_{T} (T by ERW) is the total alkalinity change due to ERW (Beerling *et al.* 2020). Kanzaki *et al.*, (2023) suggests that up to 90% of the carbon initially sequestered via enhanced silicate weathering remains stored in the ocean for 100 to 1,000 years, indicating that the ocean is a semi-permanent carbon store for human timescales and CDRs. The release of highly charged cations from basalt, along with sulfate removal via schwertmannite formation, contributes to increased seawater alkalinity. The change in alkalinity is defined by Equation 2 when described in terms of the conservative ions involved in this study. In this study, the change in alkalinity defined by Equation 2 was substituted into Equation 1 to calculate the CDR of the ocean due to ERW in the Amemasu River. The value η was set to 0.86 (Beerling *et al.* 2020).

$$\text{CDR} = \Delta \text{DIC} = \eta \times \Delta A_{\text{T by ERW}}$$

$$\Delta A_{\text{T by ERW}} = 2 \times \Delta[\text{Ca}^{2+}, \text{Mg}^{2+}] + \Delta[\text{Na}^+, \text{K}^+] - 2 \times \Delta[\text{SO}_4^{2-}]$$

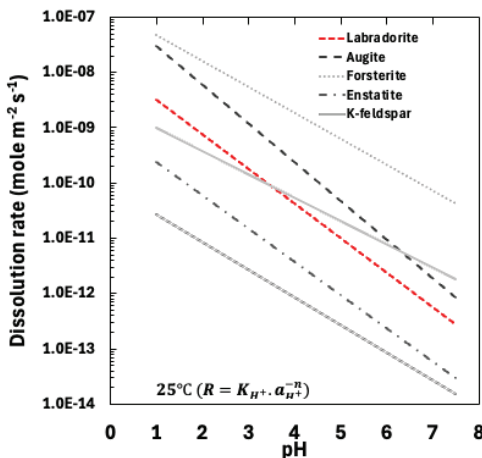


Figure 1 Dissolution rate of major minerals in basalt as a function of pH (Palandri and Kharaka, 2004; Brantly *et al.*, 2008).

Reactive Transport Modeling for basalt dissolution and CDR via ERW in AMD

A 1D-RTM was constructed to simulate alkali basalt dissolution in a flow-through system. The model was adapted from a published RTM for basalt dissolution in agricultural land (Beerling *et al.* 2020). X1t in the Geochemists' Workbench® 2023 Release 17.0 was used for modeling (Bethke, 1998). In the present calculations, only labradorite, augite, and forsterite, which are the minerals that contribute to the CDR reaction and account for 76% by weight of the alkali basalt, were considered and using kinetic parameters from Beerling *et al.* (2020). We selected these minerals because they dissolve within one year, releasing calcium and other cations.

In addition, schwertmanite, commonly observed in AMD with pH 3–4 and high sulfate concentrations (Bigham *et al.*, 1990), was included as a secondary mineral and set the kinetics data according to Sánchez-España *et al.*, 2011. The 15th of Dec. 2020 Thermoddem version of the thermodynamic database (Blanc, 2017; Blanc *et al.*, 2012) was used. We defined maximum annual basalt dissolution as the point where 99.9% of CDR-relevant minerals dissolve. Equation 3 (Beerling *et al.*, 2020) defines the dissolution rate, r_i for any mineral i . The specific surface area, a key dissolution rate variable, follows Equation 4 by assuming that the specific surface area is equal to the specific surface area calculated with a uniform 80% passing particle size (Beerling *et al.* 2020).

$$r_i = w_i \text{SSA}_i m_i \quad (3)$$

$$\text{SSA}_i = \lambda(a\rho^{-1}r^{-d-3}) \quad (4)$$

Where w_i is the mineral weathering rate, λ the roughness coefficient of the particle surface, SSA_i is the specific surface area of mineral i (cm^2/g), m_i is the mass of mineral i (g), r_i is the radius of the particle (cm), a is a geometric variable for which the particle is assumed to be spherical, d (dimension) is 2, ρ is density, 3.0 (g/cm^3) (Beerling *et al.* 2020). This study compared basalt powder (a commercial product) with basalt dust (a mining by-product from crushing and sorting). First, the 80% passing particle size of the smallest basalt product defined by Beerling *et al.* 2020 was set to 10 μm , and the 80% passing particle size was set to 10 μm for basalt products (Beerling *et al.*, 2020) and 100 μm for basalt dust, a manufacturing

by-product. The dimensions of the river were 0.5 m in height, 2.0 m in width, and variable length. Water quality parameters used in the model are presented in Table 1. These data come from laboratory analyses using inductively coupled plasma atomic emission spectroscopy (ICP-AES), inductively coupled plasma mass spectrometry (ICP-MS), and ion chromatography, as well as from field measurements of dissolved oxygen (DO), pH, and temperature.

Approach for LCA/TEA of ERW in AMD at Amemasu River

We used the LCATEA tool to calculate CO_2 emissions and costs (both operational and capital) for implementing ERW in the Amemasu River. The LCATEA tool was developed in collaboration with the National Institute of Advanced Industrial Science and Technology (AIST) using the IDEA[®] ver3.3 emissions and cost unit database of the AIST (Tahara *et al.* 2010). For this assessment, we established system boundaries including mining, crushing, and transport activities. Basalt was assumed to be dumped directly from the truck into the Amemasu River, generating no additional emissions or costs. For basalt dust scenarios, mining and crushing were excluded from calculations as dust is a manufacturing by-product. Emissions and costs were calculated by multiplying the unit, which is the emissions and costs generated in each activity, by the activity amount, which is the raw materials, energy, and travel distance used in the construction process associated with ERW on the AMD. Of the activity amounts, the amount of

Table 1 Chemistry of the AMD (Amemasu River) used in the 1D-RTM.

Species in fluid	Concentration[mg/L]	Species in fluid	Concentration[mg/L]
Ca^{2+}	15.09	$\text{O}_{2(\text{aq})}$	5.1
Mg^{2+}	2.31	Fe^{2+}	16.22
K^+	2.33	SO_4^{2-}	549.69
Na^+	4.3	$\text{Ti}(\text{OH})_{4(\text{aq})}$	1×10^{-14}
Al^{3+}	10.42	Pb^{2+}	0.101
Cl^-	6.04	$\text{H}_4\text{SiO}_{4(\text{aq})}$	20.75
As^{3-}	102.8×10^{-3}	HCO_3^-	3.16×10^{-3}
pH (-)	3.04	Flow rate (m/s)	0.19
Temperature (°C)	25		



basalt mining, crushing, and transportation is the amount of basalt that can be dissolved per year, calculated by 1D-RTM, and the transportation distance is the round-trip distance calculated from the road distance from Amemasu River to the nearest basalt mining site. A 10-ton truck was used for transport. Here, the only processes for which new construction costs were considered were mining and crushing, which may need to be newly established for ERW.

Surface Complexation Modeling of schwertmannite Adsorption in Amemasu River

To evaluate passive treatment potential, we constructed a surface complexation model (SCM) simulating arsenic adsorption over a one-month period in the Amemasu River. The model primarily examined arsenic removal through schwertmannite surface complexation, which is well known to remove arsenic from wastewater (Miyata *et al.* 2018). Khamphila *et al.* (2017) found that arsenic adsorption on schwertmannite occurs through internal complex formation, similar to adsorption on ferrihydrite. They also reported that arsenate binds more selectively than sulfate. Therefore, we used the FeOH.sdat dataset for iron hydroxide surface complexes (Bethke, 1998) in our arsenic adsorption modeling without considering sulfate adsorption, which is less competitive than arsenic. We compared arsenic concentrations in AMD treated with schwertmannite to Japanese effluent standards.

Results

Basalt dissolution and schwertmannite formation at Amemasu River (AMD)

Results illustrated in Fig. 2 show that for the 10 μm particle size, up to 900 t/year of basalt was dissolved and 191 t/year of schwertmannite was precipitated. For the 100 μm particle size, up to 400 t/year of basalt was dissolved and 108 t/year of schwertmannite was precipitated. The CDR was calculated to be 334 t-CO₂/year and 155 t-CO₂/year for the 10 μm and 100 μm particle sizes, respectively.

Net CDR(LCA) and TEA of ERW in Amemasu River

Considering the industrial process that inputs these basalt volumes into Amemasu River, the net CDR is shown in Fig. 3. Fig. 3 demonstrates the net CDR for both the 10 μm particle size product and the 100 μm particle size dust. Results indicate that the CO₂ removal by weathering is sufficient compared to the emissions in both cases. The balance between net sales and the cost of carbon credits, assuming a carbon credit price of 250 US dollars, is shown in Fig. 4. Utilizing both product and dust is economically feasible, with sufficient benefits even after considering the main operational and capital costs.

Changes in Arsenic Concentration by Schwertmannite Adsorption in Amemasu River

Fig. 5 illustrates the amount of schwertmannite formed and the change in the concentration of dissolved arsenic in the Amemasu

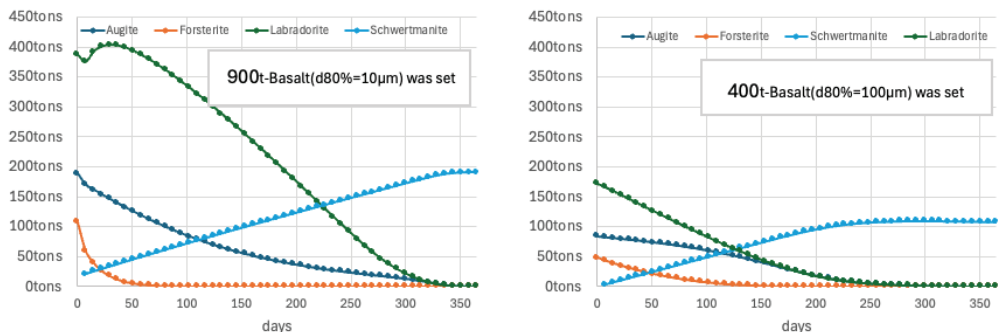


Figure 2 Annual changes in mineral contents in the alkali basalt and schwertmannite formation (900t with 10 μm particle size left; 400t with 100 μm particle size: right).

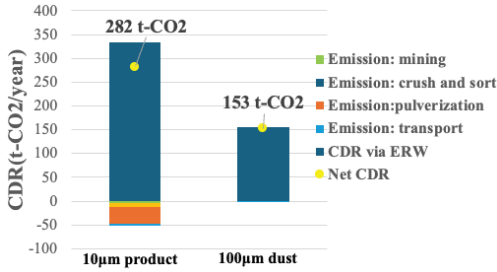


Figure 3 The balance between CDR via ERW in Amemasu River and emissions from engineering processes involved.

River due to arsenic adsorption at the amount of schwertmannite formed. When comparing arsenic removal via schwertmannite adsorption to Japanese effluent standards, the amount of schwertmannite needed to achieve the effluent standard for one month is about 8 tons. In other words, the amount of schwertmannite formed in both cases when the basalt particles to be spread is 100µm and 10µm is 12 times greater than the amount of schwertmannite needed to achieve the effluent standard for one month. This result suggests that passive treatment may be achievable.

Discussions

Our results demonstrate that the acidic conditions in AMD substantially accelerate basalt weathering, resulting in substantial net CDR, and ERW via AMD may be feasible. Furthermore, as shown in Eq. 5, the

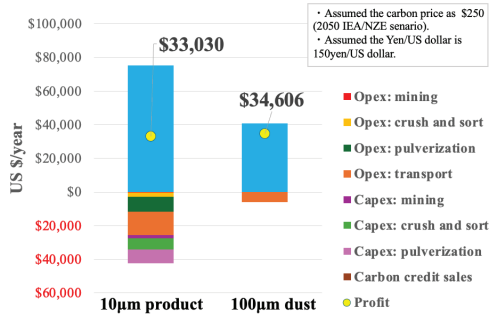
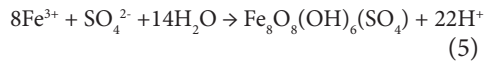


Figure 4 The balance between Sales via carbon credits assuming the price as 250 US dollars/t-CO₂ in IEA/NZE 2050 scenario and Opex/Capex of engineering processes involved.

schwertmannite-forming reaction (Schoepfer and Burton, 2021) could simultaneously supply protons and lead to large amounts of basalt dissolution by maintaining acidic conditions favorable for ERW. Results also suggest that passive treatment could be achieved for a certain period by schwertmannite adsorption. These two results indicate that passive treatment can be technically integrated with CDR via ERW in AMD.



Conclusions

This study demonstrates two main implications: the possibility of large-scale CDR and simultaneous passive treatment by AMD. These dual benefits provide substantial economic incentives, especially

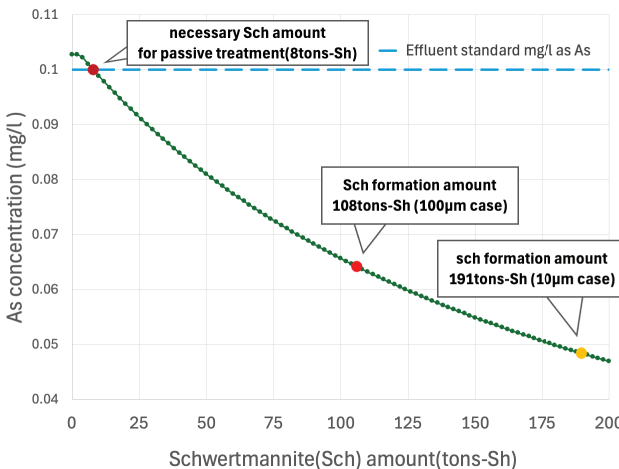


Figure 5 Arsenic concentration changes by adsorption of schwertmannite precipitated in Amemasu River.



for AMD sites dealing with arsenic, iron, and sulfate contamination. As the model has uncertainties, validation should be performed using data obtained after basalt dispersal in the Amemasu River. Furthermore, future studies should also be applied to activation treatment and compare the proposed activation treatment combined with ERW with the current active treatment in AMD treatment plants using limestone.

Acknowledgments

The paper is based on results obtained from a project, JPNP18016, commissioned by the New Energy and Industrial Technology Development Organisation (NEDO).

References

- Beerling, D.J., Kantzas, E.P., Lomas, M.R., Wade, P., Eufrazio, R.M., Renforth, P., Sarkar, B., Andrews, M.G., James, R.H., Pearce, C.R., *et al.* (2020). Potential for large-scale CO₂ removal via enhanced rock weathering with croplands. *Nature*, 583, 242–248.
- Bethke, C.M. (1998). *The Geochemist's Workbench: A User's Guide*. University of Illinois, Urbana, IL.
- Bigham, J.M. (1995). Formation mechanisms and stability of iron hydroxide-sulfate precipitates in acid mine waters. *Physica B: Condensed Matter*, 208–209, 481–483.
- Bigham, J.M., Carlson, L., Murad, E. (1990). Schwertmannite, a new iron oxyhydroxy-sulfate from Pyhäsalmi, Finland, and other localities. *Mineralogical Magazine*, 54(375), 355–365.
- Blanc, P. (2017). Update for the 2017 version. Report BRGM/RP-66811-FR.
- Brantley, S.L., Kubicki, J.D., White, A.F. (Eds.). (2008). *Kinetics of Water-Rock Interaction*. Springer, Dordrecht, Netherlands. <https://doi.org/10.1007/978-0-387-73563-4>
- IEA (International Energy Agency). (2024). *Global Energy and Climate Model*. Paris. Available from: <https://www.iea.org/reports/global-energy-and-climate-model>. Licence: CC BY 4.0.
- Kanzaki, Y., Planavsky, N.J., Reinhard, C.T. (2023). New estimates of the storage permanence and ocean co-benefits of enhanced rock weathering. *PNAS Nexus*, 2(4), pgad059. <https://doi.org/10.1093/pnasnexus/pgad059>
- Miyata, N., Akita, T., Komai, T. (2018). Arsenate adsorption and structural changes in synthetic schwertmannite: EXAFS and ATR-FTIR analysis. *Environmental Science & Technology*, 52(9), 5356–5363.
- Palandri, J.L., Kharaka, Y.K. (2004). A compilation of rate parameters of water-mineral interaction kinetics for application to geochemical modeling. U.S. Geological Survey Open File Report, 2004-1068.
- Sánchez-España, J., Yusta, I., Díez-Ercilla, M. (2011). Schwertmannite and hydrobasaluminite: a re-evaluation of their solubility and control on the iron and aluminum concentration in acidic pit lakes. *Applied Geochemistry*, 26, 1752–1774.
- Schoepfer, V.A., Burton, E.D. (2021). Schwertmannite: A review of its occurrence, formation, structure, stability and interactions with oxyanions. *Earth-Science Reviews*, 221, 103811.
- Tahara, K., Onoye, T., Kobayashi, K., Yamagishi, K., Tsuruta, S., Nakano, K. (2010). Development of inventory database for environmental analysis (IDEA). Proceedings of the 9th International Conference on Ecobalance, Nov 2010, Tokyo, Japan, 119.